SLOSHING AND SWIRLING IN MEMBRANE LNG TANKS AND THEIR COUPLING EFFECTS WITH SHIP MOTION

M Arai and **G M Karuka**, Yokohama National University, Japan
H Ando, Monohakobi Technology Institute, Japan

SUMMARY

A model experiment was carried out using an LNG carrier model with partially filled tanks and the results were compared with numerical simulations. The ship motion is calculated using the strip-method and the liquid flow computation is based on the finite difference method. The coupled behaviour between the ship motion and the partially filled tanks is studied using the measured ship motion tank horizontal forces. The tanks have a length to breadth ration near one, and because of that sloshing and swirling motions were observed during the tests. The influence of these difference modes on the coupled ship motion is discussed.

1. INTRODUCTION

When LNG carriers or Floating LNG operate with partially filled tanks, there is a possibility of violent liquid motions occurrence inside the tanks. This phenomenon is known as sloshing. Sloshing can compromise the tanks structural integrity and in order to avoid it, ships are only allowed to operate with nearly full or nearly empty conditions. In the future, however, partially loaded condition might be necessary in some operations such as LNG offloading, usage of LNG in fuel tanks, and flexibility increase on LNG logistics.

The liquid motion inside the tank may interact with the ship motion, resulting in a coupled motion. In Nam et al. [1] work, the ship motion is calculated with the impulse response function (IRF) method, and the non-linear sloshing flow is calculated with a FDM method. Regular flow was tested, and the RAO was compared with an experiment. It was found that the sloshing induced loads are not linear in respect to the motion amplitude.
Jiang et al. [2] used a similar method, but using the Volume of fluid Method interface capturing was used for solving the internal flow, and it was concluded that the coupling effects are especially larger for lower filling levels.
Hu et al. [3] studied the sloshing effect on a FLNG system, using a potential method to calculate both the ship motion and the internal flow. According to the results, the influence on pitch, yaw and heave were negligible while a noticeable effect was observed near the tank natural frequency for sway and surge.

In the present work, a model experiment was carried using an LNG carrier model with a 1:68.75 scale including forward speed, and the results were compared with numerical simulations. The ship motion is calculated using the strip-method and the liquid flow computation is based on the finite difference method. The coupled behaviour between the tank motion and the partially filled tanks is studied using the data obtained from the ship motion sensors and the bi-directional load cell installed under the partially filled tank. The tanks used in the experiment have a breadth to length ratio near one, and sloshing and swirling motions were observed during the tests.

When a partially filled tank has a length to breadth ratio near 1, there is a chance that, in addition to sloshing, a rotational flow, i.e. swirling, may also occur.
After analysing the tank dimension and arrangements of a number of LNG carriers, it was noted that some of the designs have tanks with length to breadth ratio near one. Tanks located near the aft and forward in special, tend to be shorter in order to accommodate to the hull geometry. Therefore, the problem is worth being investigated.
Swirling is a common phenomenon for spherical tanks, as described in described in Faltinsen & Timokha [4] and Arai et al. [5], for example. Swirling in prismatic tanks is mentioned when tanks are excited in irregular motion in Chen et al. [6]. Karuka et al. [7] examined the effects of swirling for regular sway excitation, identifying the conditions in which the phenomena may occur. It was found that the swirling maximum impact pressure is lower than sloshing impact pressure, but can still be significant, and the affected areas in the tank are different.

In general, there is no information available concerning the effects of swirling in coupled ship motion. Therefore, the influence of sloshing and swirling in the coupled ship motion is discussed in this paper.

2. NUMERICAL METHOD

The coupled system includes two distinct problems: the ship-motion problem and the sloshing problem. figure 1 shows a flow chart of the computation for solving the coupled ship motion and sloshing problems

2.1 SHIP-MOTION PROBLEM

The ship motion is calculated by using the strip-theory as show in equation 1.

$$(\{m_{ij}\} + \{a_{ij}\})\{\ddot{\varsigma}_j\} + \{b_{ij}\}\{\dot{\varsigma}_j\} + \{c_{ij}\}\{\varsigma_j\} = \{f_i\}_{wave} + \{f_i\}_{slosh} \quad [1]$$

Where $\varsigma_j = ship\ motions$ (1-surge,2-sway,3-heave,4-roll,5-pitch,6-yaw); m_{ij}= mass or moment of inertia; a_{ij} = added mass; b_{ij} = damping coefficients; c_{ij} = restoring coefficients; f_{wave} =wave exciting force.

- m_{ij} is the mass of the ship without liquid
- The center of gravity is calculated for the ship without liquid
- For the restoring coefficient of rolling c_{44}
- $c_{44} = m'g.GM$, where GM is the metacentric height for the ship hull without liquid, m' is the total mass including the ship and the liquid

The hydrodynamics forces and coefficients were calculated using the Strip Method. At each section of the ship, the two-dimensional radiation and diffraction problems were solved in the frequency domain by using the Boundary Element Method.
Because of the nonlinearity of the sloshing flow, the simulations are carried out in time domain. The Newmark-beta method has been employed to solve equation 1 in the time domain.

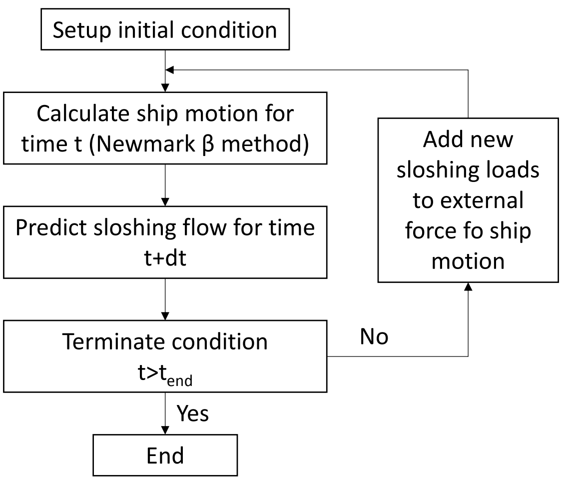

Figure 1: coupling program flowchart.

2.2 THE SLOSHING PROBLEM

The numerical method used in the analysis of sloshing was based on the finite difference technique. The numerical method is outlined below.

2.2 (a) Governing Equations

A coordinate system *o-xyz* fixed to the moving tank was adopted. Assuming an incompressible and inviscid fluid, the equations governing the liquid cargo motion inside the tank are the mass continuity equation

$$\frac{\partial u}{\partial x} + \frac{\partial v}{\partial y} + \frac{\partial w}{\partial z} = 0 \qquad [2]$$

and Euler's equations of motion:

$$\frac{\partial u}{\partial t} + u\frac{\partial u}{\partial x} + v\frac{\partial u}{\partial y} + w\frac{\partial u}{\partial z} = -\frac{\partial p}{\rho \partial x} + \frac{f_x}{\rho}$$

$$\frac{\partial v}{\partial t} + u\frac{\partial v}{\partial x} + v\frac{\partial v}{\partial y} + w\frac{\partial v}{\partial z} = -\frac{\partial p}{\rho \partial y} + \frac{f_y}{\rho} \qquad [3]$$

$$\frac{\partial w}{\partial t} + u\frac{\partial w}{\partial x} + v\frac{\partial w}{\partial y} + w\frac{\partial w}{\partial z} = -\frac{\partial p}{\rho \partial z} + \frac{f_z}{\rho}$$

Where
u, v, w: velocity components with respect to the coordinates fixed to the tank;
f_x, f_y and f_z: *x, y* and *z* components of external forces,
p: pressure,
ρ: density of the liquid.
The exciting motion of the tank is taken into account by the external forces f_x, f_y and f_z in the motion equations.

2.2 (b) Finite Difference Approximation

To reduce the computational time and to simplify the numerical method, a staggered mesh system with constant grid spacing Δx, Δy and Δz in the *x*, *y* and *z* directions was used. The variables *u, v* and *w* were evaluated at the cell faces, while p was evaluated at the center of the grid cells. Once the initial conditions of the problem were applied, the velocities *u, v* and *w* were estimated for the next time step by using the motion equations. The variables u, v, w and p were iteratively adjusted to satisfy the continuity equation and boundary conditions. Details can be found in Arai et al. [8] and Cheng et al. [9].

2.2 (c) Rigid wall

Rigid boundaries are modelled by setting zero normal velocity on the wall. Free-slip with the assumption of inviscid was used.

2.2 (d) Free Surface

The position of the free surface was evaluated by using a height function *h*, whose value was updated at every time step by applying the kinematic condition:

$$\frac{\partial h}{\partial t} + u\frac{\partial h}{\partial x} + v\frac{\partial h}{\partial y} = w \qquad [4]$$

where *h=h(t,x,y)* is the height of the free surface measured from the tank bottom and is a function of *t, x* and *y*. The atmospheric pressure p_{atm} is set at the free surface location.

2.2 (d) Impact on tank ceiling

To achieve a stable assessment of the impact pressure at the tank ceiling, a transition of the boundary condition from a free surface to a rigid wall proposed by Arai et al. [8] is considered. A detailed explanation of this condition can also be found in Cheng et al. [9].

3. EXPERIMENTAL SETUP

3.1 INTRODUCTION

An experiment was carried out at NMRI (National Maritime Research Institute) in Japan in December 2016. The goal of the experiment was to investigate the coupled behaviour of an LNG ship model and prismatic tanks filled with liquid. The ship motion and the tank internal forces were measured.

The scale between the reference ship and the model ship is 1:68.75. The force was measure though a force load cell that could measure the force in the transverse and longitudinal directions. The load cell was installed on the forward tank. Heave, sway and surge were measured by accelerometers and roll, pitch and yaw by gyroscopes.

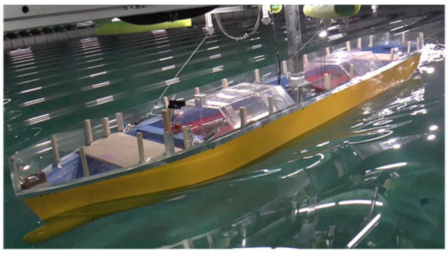

(a) LNG carrier model

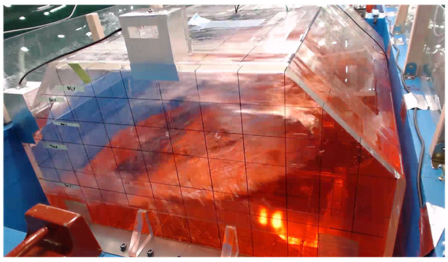

(b) Tank model

Figure 2: Pictures of the model ship and model tank.

3.2 SHIP MODEL DESCRIPTION

The model ship was designed bases on a reference LNG carrier. The LNG carrier was slightly modified for practical purposes and scaled to the model size. The model dimensions are described in table 1.

Table 1: Model ship properties.

MODEL MAIN DIMENSIONS		
Lpp	[m]	4.0
B	[m]	0.6
D	[m]	0.3
T (50%)	[m]	0.1
ROTATION CENTER POSITION		
x_c	[from AP,m]	1.9
y_c	[from center line,m]	0.0
z_c	[from keel,m]	0.1

3.3 TANK DESCRIPTION

In the ship used as reference, four LNG tanks are used. However, for practical purposes, water was used instead of LNG in the experiment. Since the water density is approximately twice as heavy as LNG, the number of the tanks was reduced from four to two in order to preserve the cargo weight between the real and the model scale. The tank dimensions are described in table 2 and figure 3. Liquid and solid tests were performed to compare the liquid effect on the ship motion. The liquid mass for each tank is 35.85kg and 60.93kg for the 30% and 50% filling levels, respectively.
In table 3, the model ship properties are described in the solid condition and in the liquid condition.

Table 2: Tank properties.

TANK DIMENSIONS			
Length		[m]	0.565
Width		[m]	0.554
Depth		[m]	0.400
Bottom chamfer height		[m]	0.056
Top chamfer height		[m]	0.121
TANK CENTER POSITION		Tank 1	Tank 2
x	[from AP,m]	2.69	1.35
y	[from center line,m]	0.00	0.00
z	[from keel,m]	0.29	0.29

*the distance from the keel to t
he tank internal bottom is 0.079m

Table 3: Test conditions.

SOLID CONDITION		30%	50%
Δ	[kg]	287.310	337.470
DRAFT	[m]	0.152	0.176
DRAFT AP	[m]	0.159	0.176
DRAFT FWD	[m]	0.148	0.176
GM_t	[m]	0.147	0.120
KG	[m]	0.162	0.174
R_{xx}	[m]	0.202	0.197
R_{yy}	[m]	0.933	0.905
LIQUID CONDITION		50% case	30% case
Δ	[kg]	287.310	337.470
DRAFT	[m]	0.152	0.176
DRAFT AP	[m]	0.159	0.176
DRAFT FWD	[m]	0.148	0.176
GM_t	[m]	0.147	0.120
KG	[m]	0.162	0.174
R_{xx}	[m]	0.213	0.215
R_{yy}	[m]	1.006	1.000
R_{zz}	[m]	1.000	0.997

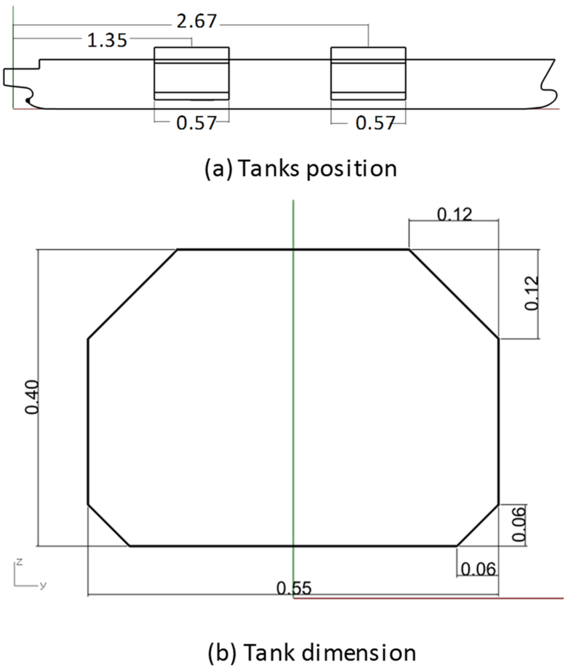

Figure3: Tank dimension and positioning

3.4 TEST CASES

Regular wave excitation was carried out including two filling levels: 30% and 50; two cargo states: solid and liquid; for a 90deg incident wave. For all cases, the ship had an advance speed of 1.117m/s. The incident wave amplitude is constant at 4cm.The first mode of the natural frequency f_1 was estimated by a linear theory suggested by Abramson et al. [10] for rectangular shaped tanks in equation 4. The estimations are shown in table 4.

$$f_1 z \frac{\sqrt{\left(g\pi/B_t\right)\tanh\left(\pi h/B_t\right)}}{2\pi} \qquad (1)$$

Table 4: natural periods estimation

Filling level	Tank Transverse T_1	Tank Longitudinal T_1
	[s]	[s]
30%	1.094	1.113
50%	0.934	0.948

4. RESULTS

4.1 REGULAR BEAM WAVES

According to figure 4 in both 30% and 50% filling conditions, the roll natural period of the ship becomes longer with the liquid cargo when compared to the solid cargo case. The T_1 of the ship goes from 1.308s to 1.613s (an increase of 0.305s) in the 50% case and from T_1=1.215s to T_1=1.616s (an increase of 0.398s). This happens due to the free-surface effect. The presence of the tanks, means that the ship has lower area restoring moment of inertia in the longitudinal direction, and hence, a longer natural period in roll. In the 30% condition, the maximum roll amplitude at the ship natural frequency is significant lower than the maximum roll amplitude in solid condition. For the 50% condition, the maximum roll amplitude is similar for both liquid and solid cases.

For sway, a local peak is observed near the tank transverse natural period. The reason for the peak is that near the tank natural period there is a 180 degrees phase inversion between the ship and the liquid motion. The local maximum corresponds to the period where the ship motion is in phase with the liquid motion. The local minimum corresponds to the period when the ship motion and the liquid motion are out of phase.
When the tank is excited in its natural frequency, the phase difference between the excitation and the liquid motion is 90deg.

For heave, no significant change is observed between the liquid and solid cargo cases., which is consistent with the results in Hu et al. [3]. Results for pitch and yaw were omitted because since the excitation is lateral, almost no response is observed.

In general, the results are very similar between 30% and 50%. However, in the 30% the influence of the liquid cargo in the roll and sway motions are clearly larger than in the 50% case. The reason is that the system the 30% and 50% conditions have approximately a 15% difference in displacement, but the internal tank force is of same magnitude near the tank natural frequency. In addition, in low filling levels, the free-surface has a larger deformation near the tank natural period, because non-linear effects are larger.

4.2 FORCE MEASUREMENT

The forces were measured in a load cell mounted on the forward tank. model. The forces were measured in local coordinate system, which rotates in roll, pitch and yaw with the ship.
We can see that near the tank natural period, when sloshing or swirling occurs, there is an increase in the measured forces. The large transverse force measured near the ship's natural period is due to the large roll inclination of the model. When the model is inclined, the liquid pressure on the tank is high, although the free surface moves slowly.

The forces were converted to a global coordinate system fixed parallelly to the still free-surface and then compared with numerical results. The transverse force of the slow free-surface movement in the global coordinate system is small because the force exerted to the tank is the liquid weight (vertical force), and hence the horizontal forces are small. Choosing the global coordinate system to show the results emphasize the forces generated by dynamic forces in the liquid motion rather than the forces generated by the liquid weight.

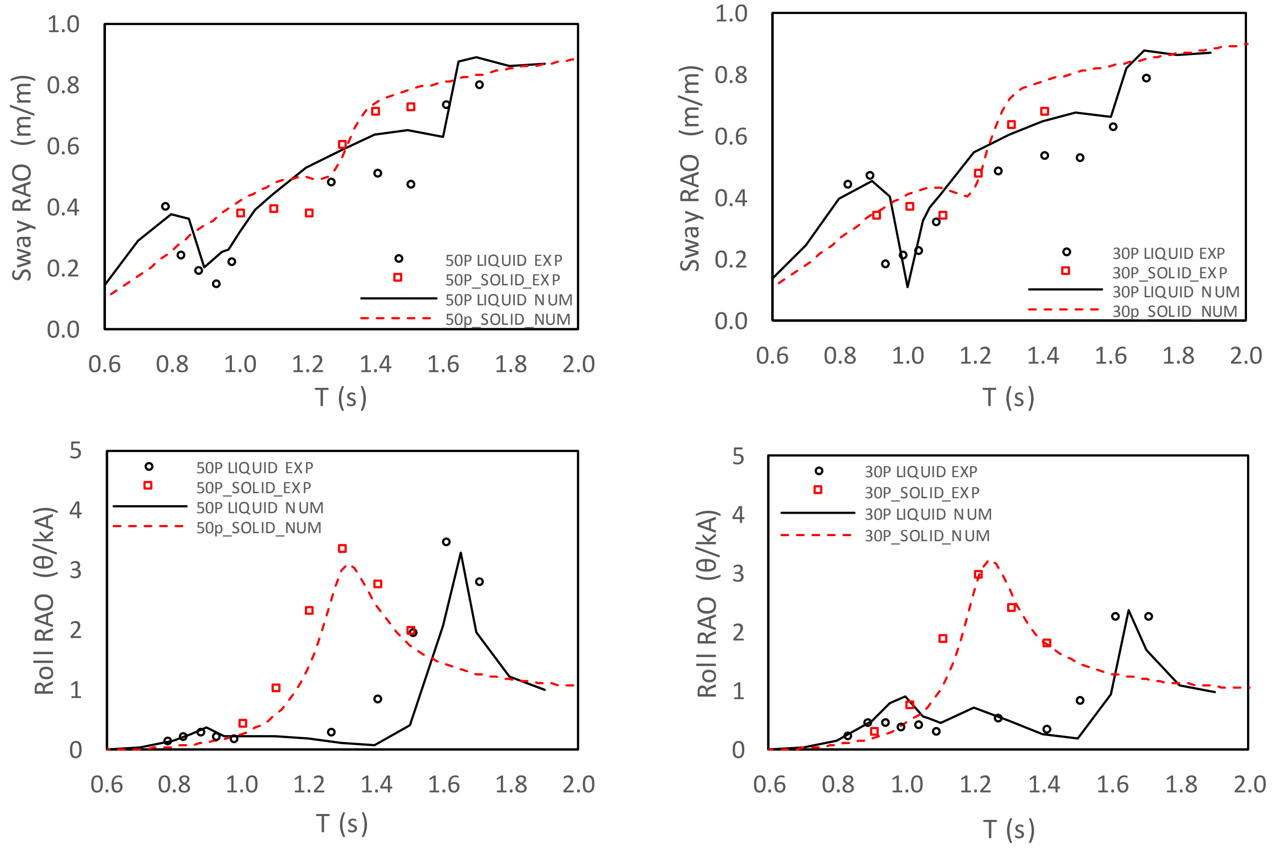

Figure 4 – RAO for 50% (left) and 30% (right) filling levels, beam sea

It can be seen in figure 6 that the sloshing and swirling happens near the tank natural frequency.
When transverse sloshing occurs, there is a sharp increase in the transverse force. When swirling occurs, there is an increase in both F_x and F_y.

Although the force comparison shows good agreement when dynamic effects are small, there are significant difference in the result near the tank natural period. It can be noted that the liquid effect on the ship motion can be predicted with reasonable accuracy, but the opposite is not true. The sloshing mode or swirling mode is very sensitive to the tank excitation.

In general, the comparison between F_y is reasonably predicted. However, F_x results has considerable differences. Such disparities were observed when different modes occurred. For example, in some cases in the experiment swirling occurred, while in the simulation sloshing occurred. When the tank is excited only in sway direction. The occurrence of swirling can be identified by checking the relation between F_x and F_y. When F_y is large and F_x is low, transverse sloshing is occurring. When both F_x and F_y are large, swirling is occurring.

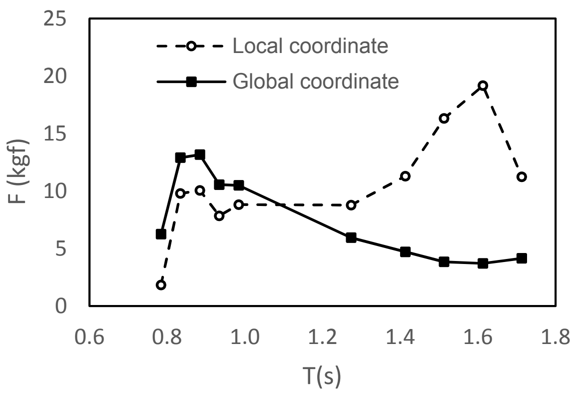

Figure 5: Forces in local and global coordinate systems

When T_1=0.934s, swirling occurs, and both F_x and F_y are excited, having almost the same magnitude and with a phase difference of 90 degrees. The phase diagram has a circle shape.
When T_1=0.984s, transverse sloshing occurs, the transverse force is predominant, and the diagram phase has the shape of a narrow ellipse.

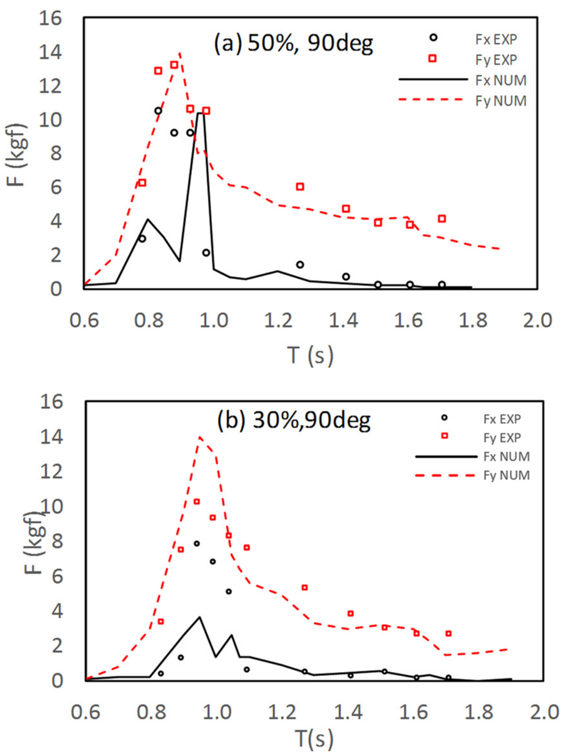

Figure 6: Measured forces in global coordinates

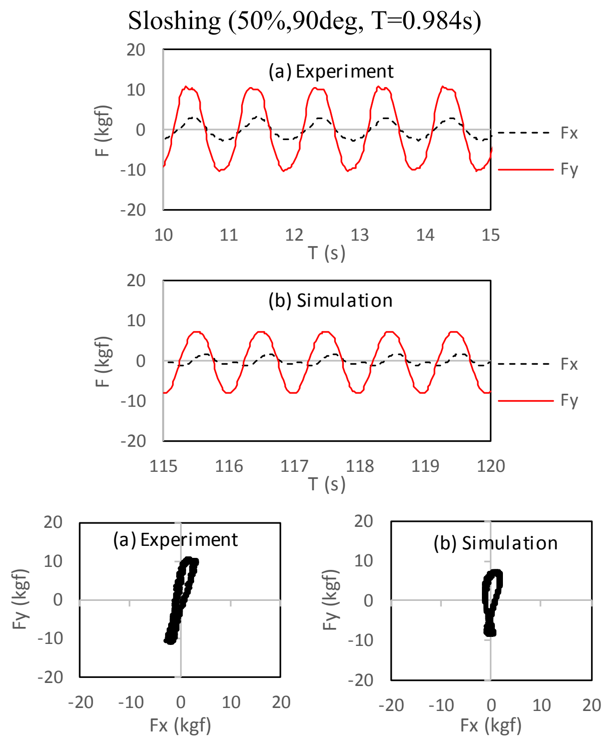

Figure 7: comparison between simulation and experiments for sloshing and swirling

Figure 7 shows the cases where T= 0.934s and T=0.984s, respectively, are shown.

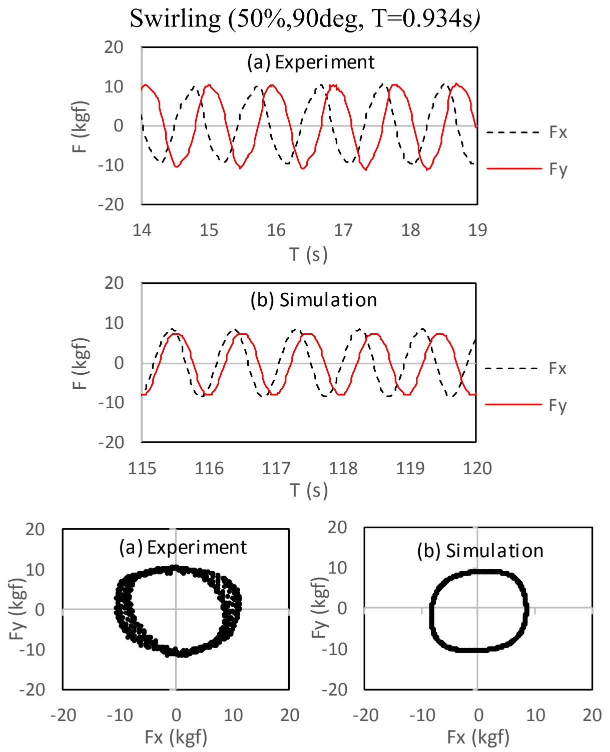

4.4 INFLUENCE OF SLOSHING AND SWIRLING IN THE COUPLED SHIP MOTION

The case described in figure 7 shows swirling occurrence in the counter-clockwise direction. In the experiment, the rotation did not have a preferential direction, with both clockwise and clockwise swirling occurring. It is believed that small disturbances, such as deformations in the initial free-surface can trigger the rotation in one direction or the other.

In the simulation, it is possible in some cases to control the rotation direction by adding artificially a small inclination angle to the initial free-surface. An initial -2.0deg and a 2.0deg inclination around the y axis resulted in a counter clockwise and clockwise rotation, respectively.

In order to understand the effects of the rotation direction on the tank forces and the coupled motion, both cases were investigated. In addition, in order to compare the swirling effects to the sloshing effects, a third case where the tanks are 10% longer were also included. With a longer tank, only sloshing occurs. The liquid density of the computation liquid was adjusted to keep the liquid mass constant.

Figure 8 shows that depending on the rotation direction, the maximum force on the longitudinal direction is different. As expected, the longitudinal force for the transverse sloshing case is minimum. The transverse force F_y have nearly the same magnitude and phase for all the three cases.

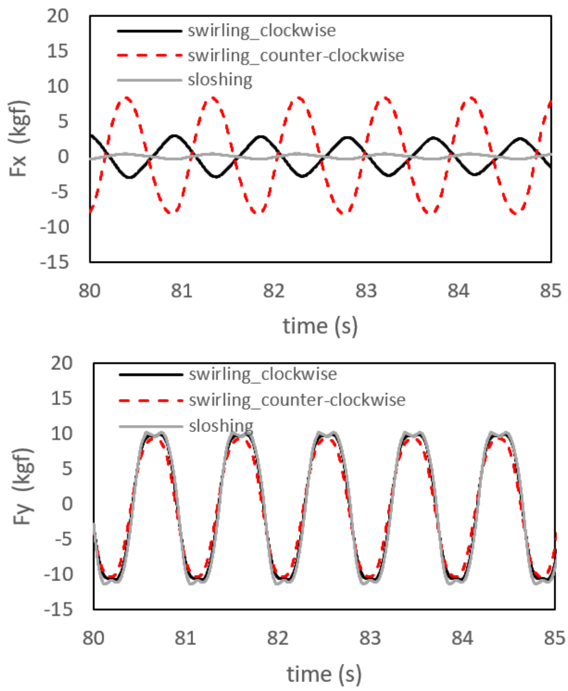

Figure 8: tank forces for different sloshing and swirling for 50% filling level, beam wave, T=0.934s.

In terms of coupled ship motion, the yaw and pitch motions are very small for beam waves and the heave has almost no influence from the liquid motion, so only sway and roll are shown in figure 9. Not a large variation is observed, but in terms of sway, the sloshing case is about 20% lower than both the swirling cases, whereas in terms of roll, the swirling in counter-clockwise is about 9% lower than sloshing and the clockwise swirling.

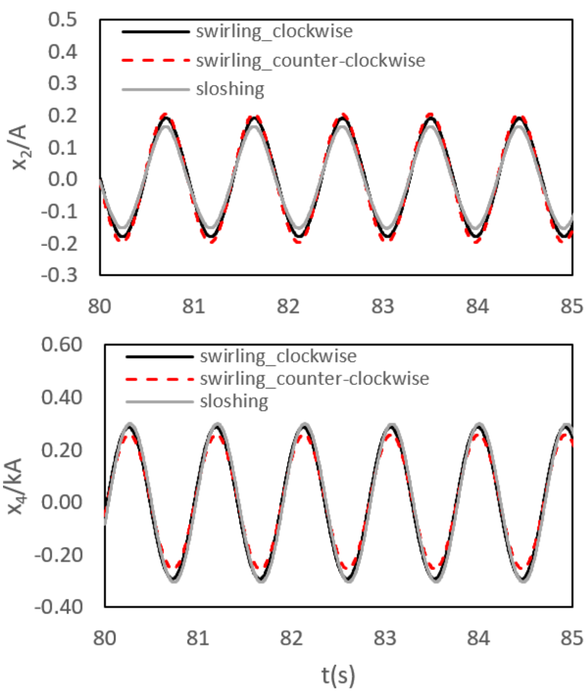

Figure 9: effect of sloshing and swirling on the coupled ship motion for 50% filling level, beam wave, T=0.934s.

5. CONCLUSIONS

A numerical method was developed to estimate the coupled behaviour of a ship and its internal tanks. A reasonably accurate prediction of the ship motion was obtained. The results are consistent with the results from different experiments and researches. The main effects of the liquid motion in the ship motion are: 1. The roll natural period becomes longer due to the free-surface effect. 2 A local roll peak occurs near the tank natural period which can be considerably large. 3 A small local peak appears in sway near the tank transverse natural period due to phase difference between the ship motion and the liquid motion. 4 No significant effect is observed on heave and pitch.

On the other hand, the liquid motion inside the tank showed significant difference between the measured and calculated forces, which suggests that slight differences in motion prediction can lead to significant differences in the liquid motion prediction. The prediction becomes especially difficult when the tank has breadth to length to ratio near 1, which is the case where both sloshing and swirling may occur. When the same mode occurred in the experiment and simulation, the force measurements were consistent.

The results show that the coupled behaviour is different when sloshing or swirling occurs. Moreover, the coupled behaviour is also dependent on the swirling rotation direction. The rotation direction did not show a constant pattern. The rotation direction is random or very hard to predict, and it strongly dependent on the initial free-surface condition.

6. ACKNOWLEDGEMENTS

Part of this research was carried out as ClassNK's Joint R&D with Industries and Academic Partners project. The authors would like to express their gratitude to ClassNK for their support.

7. REFERENCES

1. Nam B.W., Kim Y., Kim D.W., Kim Y.S., 'Experimental and Numerical Studies on Shi Motion Responses Coupled with Sloshing in Waves', Journal of Ship Research, Vol. 53, pp68-82, 2009

2. Jiang S.C., Teng B., Bai W., Gou Y., 'Numerical simulation of coupling effect between ship motion and liquid sloshing under wave action', Ocean Engineering 108, p140-154, 2015

3. Hu Z.Q., Wang S.Y., Chen G., Chai S.H., Jin Y.T, 'The effects of LNG-tank sloshing on the global motions o FLNG system', International Journal of Naval Architecture and Ocean Engineering 9, p114-125, 2017

4. Faltisen, O.M., Timokha A., 'Nonlinear sloshing in a spherical tank', Conference Proceedings, OMAE, 2013

5. Arai M., Cheng L.Y., Wang X., Okamoto N., Hata R., Gustavo M.K., 'Sloshing and swirling behavior of liquid in a spherical LNG tank', Proceedings of International Symposium on Ships and Other Floating Structures PRADS, 2016

6. Chen B.F., Wu C.H., 'Effects of excitation angle and coupled heave–surge–sway motion on fluid sloshing in a three-dimensional tank', Journal of Marine Science and Technology, Vol. 16, Issue 1, pp. 22–50, 2011

7. Karuka G.M., Arai M., Yoshida T., Cheng L.Y., Ando H., 'Swirling effects and occurrence in chamfered prismatic tanks with partially filled loaded condition', Journal of the Japan Society of Naval Architects and Ocean Engineers., 2017

8. Arai M., Cheng, L. Y., Kumano, A., Miyamoto, T., A., 'Technique for Stable Numerical Computation of Hydrodynamic Impact Pressure in Sloshing Simulation', Journal of the Society of Naval Architects, Japan, Vol. 191, pp. 299-307, 2002

9. Cheng, L. Y., Arai, M., 'A 3D Numerical Method for Assessment of Impact Loads Due to Sloshing in Liquid Cargo Tanks', Proceedings of the Fifteenth International Offshore and Polar Engineering Conference, pp. 214-221, 2005

10. Abramson H. M., Bass R. L., Faltinsen O.M., Olsen H.A., 'Liquid Slosh in LNG Carriers, 10th Naval Hydro-Dynamics Symposium', pp.21-38, 1974

8. AUTHORS BIOGRAPHY

M Arai is a Professor at Yokohama National University. His previous research topics include Study on 3D Sloshing Simulation and Study on an anti-sloshing device for the tanks of LNG carrier and FLNG

G M Karuka is a doctoral course student at Yokohama National University. His previous experience includes the occurrence of swirling in prismatic tanks.

H ANDO is a Senior General Manager at Monohakobi Technology Institute.